

Musca domestica inspired machine vision sensor with hyperacuity

To cite this article: D T Riley *et al* 2008 *Bioinspir. Biomim.* **3** 026003

View the [article online](#) for updates and enhancements.

You may also like

- [Reconfigurable Battery Pack for a Lithium Based Battery Charger for BMS Applications](#)
Larry Morris, Mark H Weatherspoon, Jamal Frederon Stephens et al.
- [Optimization of the SPECT systems based on a CdTe pixelated semiconductor detector using novel parallel-hole collimators](#)
Y -J Lee, S -J Park, D -H Kim et al.
- [Reconfigurable Battery Pack for a Lithium Based Battery Charger for BMS Applications](#)
Larry Morris, Jamal Frederon Stephens, Pedro L. Moss et al.

Musca domestica inspired machine vision sensor with hyperacuity

D T Riley¹, W M Harmann¹, S F Barrett² and C H G Wright²

¹ Sensors and Platform Branch, Naval Air Warfare Center, China Lake, CA, USA

² Department of Electrical and Computer Engineering, College of Engineering and Applied Science, University of Wyoming, 1000 E University Avenue, Dept 3295, Laramie, WY 82071, USA

E-mail: steveb@uwyo.edu

Received 2 October 2007

Accepted for publication 20 March 2008

Published 25 April 2008

Online at stacks.iop.org/BB/3/026003

Abstract

A fiber optic sensor inspired by the compound eye of the common housefly, *Musca domestica*, has been developed. The sensor coupled with analog preprocessing hardware has the potential to extract edge information quickly and in parallel. The design is motivated by the parallel nature of the fly's vision system and its demonstrated hyperacuity or precision of visual localization beyond the conventional resolution limit. The fly's anatomy supporting the design is reviewed, followed by the design of a one-dimensional, cartridge-based sensor. The sensor's ability to locate a line stimulus in a two-dimensional space is demonstrated. Discussion is provided to extend this work in scale, cartridge dimension, information and array processing.

(Some figures in this article are in colour only in the electronic version)

1. Introduction

The early vision system of the common housefly (*Musca domestica*), as well as many higher level organisms, exhibits interesting aspects such as cellular preprocessing, parallel structure and high resolution. These features may be mimicked in sensor technology to allow for the rapid extraction of image primitives: object edges, boundaries, image segmentation and movement parameters. We define early vision as the vision processes that occur within the first few cellular synapses beyond the photoreceptor layer. This analog, parallel approach to vision provides advantages over most current electronic imaging systems that digitize the spatially sampled pixel information early in the signal path. The same type of object information can be extracted with a digital-based system; however, extraction usually requires multiple passes of image processing techniques that must be exhaustively applied pixel by pixel to an image. A fly-inspired, analog-based sensor can be useful for imaging applications that are currently difficult or computationally expensive using traditional image processing techniques. Furthermore, some applications might optimally employ a hybrid approach using both technologies.

We have divided our biomimetic computer vision research efforts into the following categories: electrophysiology of

the fly's vision system; ongoing system modeling using a MATLAB coded, multi-sensor (>10 000), video-based simulation; physical sensor development and application development. In this paper, we concentrate on the development of a physical sensor to extract the location and position of a line stimulus within the field of view (FOV) of a one-dimensional fly-inspired sensor. We begin with a brief review of limitations of traditional digital-based machine vision, followed by a brief review of the fly's vision system apropos to this research effort. We then discuss the development and testing of a physical sensor. We conclude the paper with a discussion of results and our future research plans for sensor development.

2. Background

2.1. Digital-based machine vision processing

Modern machine vision systems typically contain three major components: a camera containing sensor array (such as a charge coupled device (CCD) array), a frame grabber to convert the CCD information into a useable two-dimensional array of gray or color-scale pixel data representing the captured image, and a host processor to extract pertinent information

from the digitized image. The CCD sensor comprised a rectangular array of individual photo detectors which converts impinging photons into a usable electrical signal. For sampling-limited systems, increased resolution implies more pixels, and thus comes at the cost of more data that must be transmitted to the main processor. These data may be sent serially (one bit at a time) for the most basic frame grabbers or with serial interface devices that utilize USB or Firewire; however, alternate devices may transmit in parallel (32 bit transfers are common). Some of the fastest common methods for transferring data between digital devices are capable of speeds in excess of 400 Mbps (million-bits-per-second) [1]. Depending upon the specific application, the digitally rendered image may then be filtered, edge detected, segmented, etc, to extract the features or information of interest from the image. These operations often require multiple passes of time-consuming pixel-by-pixel processing, taking a large number of CPU clock cycles. In certain time-sensitive or CPU-limited applications, a digital-based approach may not be practical.

2.2. *Musca domestica* vision

The goal of our research is not to exactly reproduce the form and function of the fly's vision system. Instead, we mimic selected features and characteristics that prove useful in sensor development and image processing. The vision system of the common housefly and other dipterans exhibit a highly parallel, compartmentalized, analog vision system. The primary visual system of the housefly consists of two compound eyes that exhibit neural superposition. Each eye contains approximately 3000 ommatidia, the major modular structural unit of the eye. A single ommatidium consists of a 25 μm facet lens followed by a cone-shaped lens and a complement of photoreceptors as shown in figure 1. The photoreceptors (R1–R6) are arranged in an almost circular fashion. Two other photoreceptors designated R7 and R8 lie inside the pattern, one above the other, and are connected directly to the medulla [2–5]. The major function of the photoreceptors is to act as transducers which convert light energy or photons into an ionic current. The photoreceptors are sensitive to the magnitude and angle at which the light approaches. This angular sensitivity has a very distinct profile that is approximately Gaussian [2, 6–8].

Each photoreceptor is connected, along with common view photoreceptors from adjacent ommatidium, to the monopolar cells L1 and L2 forming a structure known as the 'cartridge'. While these photoreceptors for a given cartridge share a nearly identical view of the same point in distant space (i.e. in the far field), there is a slight displacement which results in overlapped Gaussian profile responses as shown in figure 2. These overlapping signals are combined and preprocessed by the L1 and L2 monopolar cells. The exact function of the L1 and L2 output is not entirely known. While some researchers hypothesize that they could be encoded signals containing position information [9], others disagree [10, 11]. Douglass and Strausfeld have concluded that the responses of L1 and L2 to motion and flicker are indistinguishable at equivalent contrast frequencies and are therefore not motion specific [12]. Juusola and French have

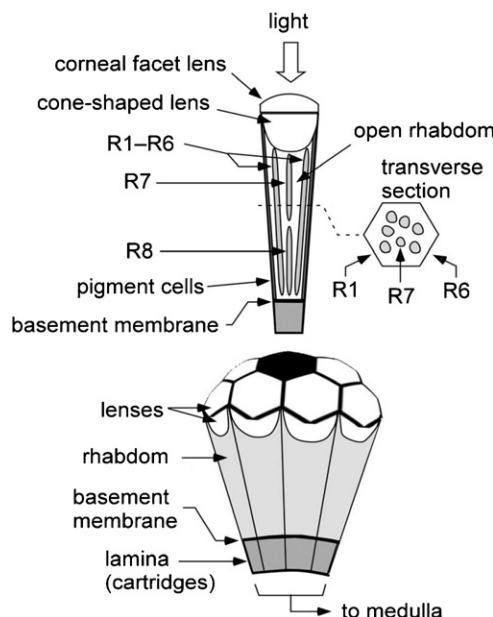


Figure 1. A single ommatidium consists of a 25 μm facet lens followed by a cone-shaped lens and a complement of photoreceptors. The photoreceptors are arranged as shown in the cross section. Two photoreceptors (R7 and R8) are connected directly to the medulla.

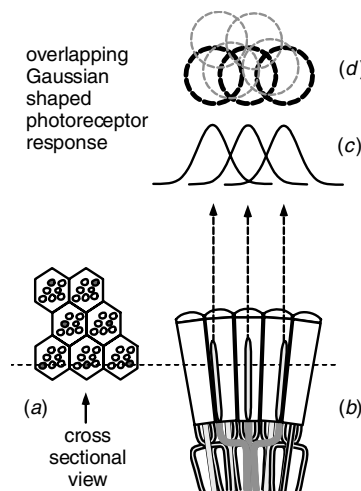


Figure 2. Each photoreceptor is connected, along with common view photoreceptors from adjacent ommatidium (a), to the monopolar cells L1 and L2 forming a structure known as the 'cartridge' (b). While these photoreceptors share a nearly identical view of the same point in distant space (i.e. in the far field) (c) there is a slight divergence which results in Gaussian profile overlapped responses (d).

concluded that the large monopolar cells 'improve the ability of the eye to detect moving objects by compressing the wide range of photoreceptor responses at different light levels to a narrower range' [8].

A third monopolar neuron found in the cartridge, L4, is connected distally to the L1 and L2 monopolar cells and proximally to neighboring cartridges. L4 is thus capable of transmitting information encoded by the L1 and L2 monopolar

cells to neighboring cartridges [4, 5, 11–13]. This analog communication network is thought to provide the foundation necessary to perform much of the preprocessing required to reduce an image into its salient features. Because this processing is performed in the retina and lamina, using only a small number of neurons rather than the medulla, it is equivalent to a real-time analog preprocessing stage and is thought to be responsible for much of the speed and accuracy of the fly's vision system [10]. There are other cells within the cartridge, and their exact function remains under investigation. van Hateran and Stavenga *et al* have accomplished a large body of work studying the vision system of related species. Specifically, they have investigated optics, coupling mechanisms and system response to varied stimuli [14–21].

2.3. Hyperacuity

Houseflies are capable of resolution greater than that implied by the photoreceptor spacing of the retinal array, a phenomenon known as *hyperacuity* [9]. Nakayama defined hyperacuity 'as a precision of visual localization beyond the resolution limit' [22]. Hyperacuity in a neural superposition compound eye is possible because each photoreceptor that projects into a cartridge shares a common visual axis and thus views an overlapped sample of the same point in space [23–25]. Pick showed that the photoreceptors do not share precisely the same visual axis. Instead they are slightly 'misaligned' [24]. We hypothesize that the fly would not maintain such alignment if the eye could not make use of the advantage gained by the disparate photoreceptor axes [25]. Measurements by Snyder *et al* further support this hypothesis. They have measured the optical quality of many animals and found that the modulation transfer function (MTF) is 10 to 100 times better than it has to be to match the spacing of the photoreceptor matrix [6]. It is notable that the value of the improved optical quality matches the animals' observed behavioral performance, suggesting that they actually use the high resolution information for vision [25]. Also, Bucklew and Saleh indicate that the actual practical limit for resolution is the contrast limit [26]. This biological evidence, while not conclusive, encouraged our development of a new sensor based on the early layers of the fly's vision system.

While the responses of *Musca domestica* are Gaussian, it should be noted that hyperacuity can be achieved with other types of continuous, nonlinear function. Figure 2 shows the overlapped Gaussian curves representative of a response to an object crossing the fields of view (or response lobes) of three photo elements in one dimension.

When using multiple common view photoreceptors such as those found in *Musca domestica*, the overlapping signals can be used together to determine the precise position of an object within a sensor field of view. When an object is stationary within any of the multiple element lobes, one or more photoreceptors output a constant signal dependent upon the object position. Comparison of the magnitudes of the photodetector signals provide enough information to determine the precise position of an object such as a line stimulus.

2.4. Information sharing between ommatidia

As previously mentioned, the fly's vision system has 3000 independent ommatidia collecting image information in parallel. Previous research on optomotor response and cellular interconnectivity suggest that the ommatidia share information from their neighbors to perform coordinated, higher level image processing tasks. Hartline, Wagner and Ratliff (1956) demonstrated that the outputs of ommatidia interact with one another through a process of lateral inhibition between neighboring photoreceptors [27]. Reichardt (1961) determined that the motion processing behind the optomotor response in insects was mediated by local interactions between adjacent ommatidia and developed a classic model of motion based on this interaction [28]. It is unresolved in the literature as to the exact underlying cellular structure for ommatidia interaction. However, the L4 monopolar cell has three collateral connections to three different cartridges, one of which is the parent cartridge of the neuron. This provides an individual ommatidium with the ability to share information with its neighbor as well as compare present output to previous output (made possible by temporal delays between certain cellular connections).

2.5. Early vision processes

Several research groups have performed outstanding work in investigating the vision processing of the common housefly [29–39]. Space does not allow an exhaustive review of this body of work. We limit our discussion to some of the findings most relevant to this study. Specifically, we address previous research relative to processing in the first cellular synapses in the visual system. We believe from an engineering standpoint that there is considerable visual information to be gleaned from the photoreceptors and their interaction with the first several cellular layers, and our work has replicated much of this in sensor hardware. In addition, we briefly mention the work of other research groups investigating higher processing centers in the fly's vision system for completeness. The interested reader is referred to [22] for a historical literature review.

Past researchers studying single unit recordings in various organisms found visual neurons which had sensitivity to moving images [40–42]. These researchers noted that the impulse rate of specific cells were modified by changes in the stimulus direction. Even higher order vision processing tasks may be possible in the early vision system (i.e. prior to the visual cortex). Marr noted in his landmark work 'Vision' that primitive but vital forms of object recognition may take place on the retina. He further noted that a single neuron can perform much more complex and subtle tasks than had been previously thought, such as to detect pattern elements, discriminate the depth of objects, etc [43]. He based these conclusions on the early work of Barlow on frogs. Barlow observed the selectivity of the retinal neurons and the frog's reaction time when they are selectively stimulated, suggesting that they are bug detectors performing a primitive but vitally important form of recognition on the retina [40, 43]. Work by Nakayama and Loomis (1974) also supported the belief of sophisticated processing occurring at the retinal level. They noted that

center-surround motion detectors (cells insensitive to uniform motion over the center and surround) are highly sensitive to velocity differences between the center and surround [44]. O'Carroll further noted that insects possess neurons that are tuned for detecting specific pattern features such as oriented line edges and moving spots [45]. Various algorithms have recently been developed to describe motion processing in the fly at the ommatidia level. It is believed that the fly eye perceives details of images as a result of uneven excitation of different ommatidia at the same time. However, another type of perception of detail has recently been proposed based on the uneven excitation of the same ommatidium at different times. This model implies that the eye has some kind of 'memory' element that allows comparison of previous retinal excitation with a subsequent one [46]. As previously noted, there are several cellular feedback mechanisms in the literature that support this hypothesis. Zheng *et al* investigated the role of feedback synapses. They demonstrated that the feedback synapses form a negative feedback loop that controls the speed and amplitude of photoreceptor responses and hence the quality of transmitted signals. Furthermore, Zheng noted that ultrastructural studies have shown a complex arrangement of feed forward and feedback synapses that use a diverse array of excitatory and inhibitory transmitters. Processes are linked together and to adjacent cartridges with thin extending fibers suggesting that each process could be a locally interacting element, which may see only a limited activity from other such segments in the same or neighboring cartridges [47].

2.6. Higher order processing

Extensive work has been accomplished on vision and motion processing within higher order process regions of the fly's vision system. Nakayama summarizes four different types of motion processing models based on elementary motion detectors (EMDs). Most notably, Reichardt ascertained that the motion processing underlying the optomotor response in insects was mediated by local interactions between adjacent ommatidia [48]. Reichardt presented a computational model employing the principle of autocorrelation which still remains an important general theory of motion processing. Srinivasan also found directionally sensitive cells in the fly's lobular plate [49], while Bishop reported classes of directionally sensitive motion detecting units [50]. As mentioned previously, van Hateran and Stavenga *et al* have accomplished a large body of work studying the vision system of related species. Specifically, they have investigated optics, coupling mechanisms and system response to varied stimuli [14–21].

3. Previous sensor work

There are three basic configurations of compound eyes: apposition, optical superposition and neural superposition [51–53]. In apposition eyes, pigment cells surround the ommatidium so light is received down the central ommatidial axis. In optical superposition eyes, the pigment is not present so insects are able to collect light from a variety of directions. This increases the sensitivity of the eye while reducing

its resolution. In neural superposition eyes, the cartridge is equipped with the interommatidial pigment, but light is collected from adjoining cartridges as previously discussed [51–53]. Several research groups have developed artificial apposition compound eyes [54–56]. Currin developed a system based on an apposition eye. He used three gradient index (GRIN) lens and their overlapping fields of view to develop a point tracker designated the multi-aperture vision system (MAVS) [57]. Jeong has developed techniques to manufacture a 3D compound eye on a spherical surface using microlens technology [56]. Rosen and Abookasis have employed neural superposition principles to image bones hidden within biological tissues [55]. Tanida *et al* developed a compact image-capturing system designated TOMBO for thin observation module by bound optics. This system uses compound-eye imaging optics to capture a number of images that are then rendered to retrieve the image of the object [58–60]. Hoshino *et al* have developed an insect-inspired micro-fabrication technique which combines a microlens array, photo-diode array and an electrostatically driven scanning slit on a single chip. This system can detect a contrast with high temporal resolution [61]. Our current work falls into the category of a neural-superposition-based sensor.

Harrison has compiled a noteworthy body of work on the fly's flow field processes. Harrison studied the system in detail and rendered silicon flow field generators inspired by the fly [62–65]. He stated that 'optic flow is a computationally demanding task because, like early vision tasks, it involves operations that must be performed identically on every pixel of an image. Local estimates of motion must be laboriously computed before the overall pattern is analyzed. This task is ideally suited for parallel computation. If we divide the job to many processors, each dealing with one pixel and communicating with its immediate neighbors, the task becomes much easier'. Harrison developed a single-chip analog VLSI sensor that detects imminent collisions by measuring radially expanding optic flow based on the delay-and-correlate scheme similar to that first proposed by Reichardt (1956) [62–65]. Pudas *et al* have also developed a bio-inspired optic flow field sensor based on low temperature co-fired ceramics (LTCC) technology. The LTCC technology provides reliable, small profile optic flow sensors that are largely invariant to both contrast and spatial frequency [66].

With this brief review of previous related work complete, we now describe our efforts toward designing a sensor based on the early vision processes in the fly's eye.

4. Methods

In order to design a sensor based on the vision system of the common housefly with the key attribute of hyperacuity, we investigated the optical design, electronic processing and sensor housing design of a one-dimensional sensor consisting of three photo elements with overlapping Gaussian profiles. Each design area will be discussed in turn.

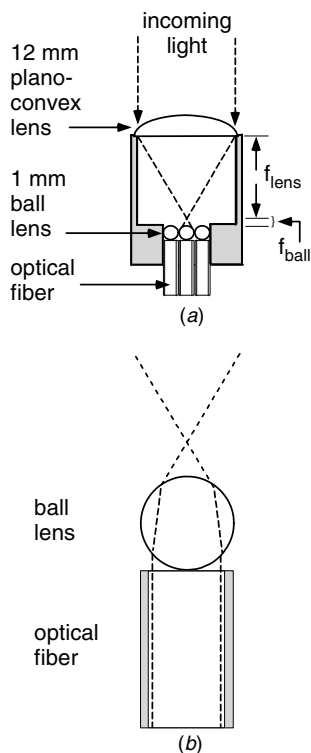


Figure 3. (a) The basic sensor configuration consists of a plano-convex lens shared by three 1 mm optical fibers, each equipped with a 1 mm ball lens. (b) The three fibers are such that the lens' focal point was at the effective focal point of the center ball lens.

4.1. Optical design

The basic optical design of the sensor consisted of a common lens focusing light onto an arrangement of photodetectors similar to the configuration found in the fly's eye as shown in figure 3(a). To make the system functionally similar to the fly, we needed to produce electrical signals with an angular sensitivity that was Gaussian in form and would possess the correct amount of overlap between adjacent sensors.

The biological response data collected in *Musca domestica* research and the known anatomy of the fly provided an estimate of the amount of overlap present in the fly eye. The goal of this design was to obtain $75\% \pm 5\%$ overlap of Gaussian responses [9]. Further overlap was limited by the physical spacing of sensor optics for this configuration. Research has shown *Musca domestica* to have overlapping responses as high as 90% [24].

To achieve the desired Gaussian overlapped response, three 1 mm diameter jacketed fiber optic light guides [67] were mounted adjacent to one another. The polished end of each fiber was equipped with a 1 mm ball lens as shown in figure 3. The interaction of light between the acceptance angle of each ball lens coupled to the core by the optical fiber provides the desired Gaussian profile for a given photoreceptor. The close proximity of the ball lenses provides for the overlapping Gaussian profile. The three fibers were mounted behind a plano-convex lens ($d = 12\text{ mm}$, $f = 12\text{ mm}$) such that the lens

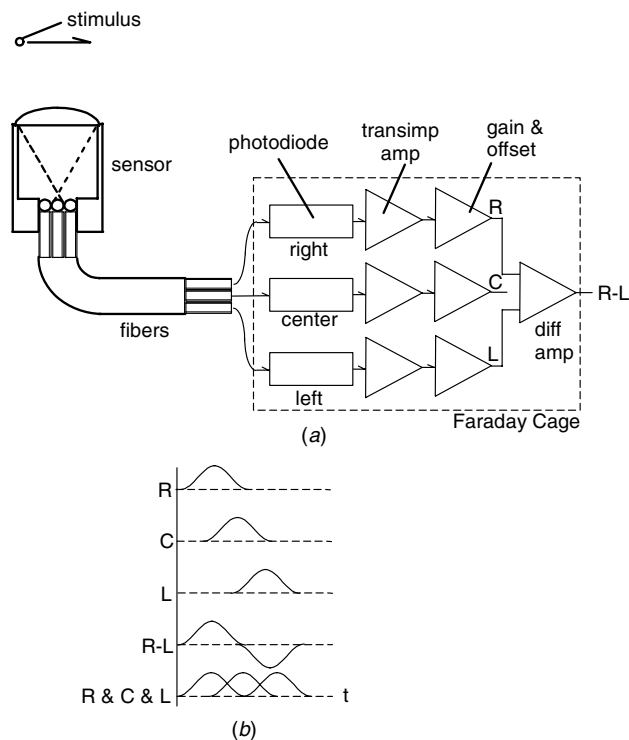


Figure 4. The output from each optical fiber is fed to a photodiode/transimpedance amplifier monolithic device followed by a single operational amplifier stage to provide gain and offset. Construction of the analog hardware within a Faraday cage minimizes noise effects. Additional processing is required to extract the stimulus range. (a) Analog hardware and (b) signal response to a stimulus moving left to right in sensor FOV.

focal point was at the effective focal point of the center ball lens [68–71], as shown in figure 3(b). The other end of each fiber was terminated with an Advanced Optoelectronic Solutions (TAOS) TSL250R light-to-voltage optical sensor mounted within fiber sensor coupling [68], as shown in figure 4. Harman has described the field of view for specific sensor configuration based on the characteristics of the plano-convex lens (diameter and focal length), the ball lens diameter and the diameter of the optical fiber using geometric ray tracing principles [73]. For the specific physical configuration described, the individual photoreceptor field of view was approximately 60° while the overall cartridge field of view was 22.6° [74].

4.2. Analog preprocessing

In selecting a photodiode, spectral responsivity, response time, angular sensitivity, active capture area and packaging were all taken into consideration. Because the housefly sees primarily in the visual wavelengths and this was also our own region of interest, a photodiode with maximum responsiveness between 390 and 780 nm was employed. The TAOS TSL250R light-to-voltage converter was chosen as it contains a monolithic combination of a photodiode and a transimpedance (current-to-voltage) amplifier circuit and its high sensitivity. The off-the-shelf TSL250R is equipped with a half ball lens, which was filed off for this application. The output from the photodiode

was connected to a single stage non-inverting operational amplifier configuration to provide variable gain and offset as shown in figure 4. The variable gain allowed the output from each photodiode to be matched to one another.

4.3. Fiber and lens housing

A single-piece sensor housing was designed to provide a rigid structure for the sensor. By making the housing a one-piece part and placing a large tapped screw hole in the top of the housing directly above the fiber slot, it was possible to use a nylon screw with a flat tip to hold the fibers in place. This solution allowed for easy replacement of fibers as necessary. The design was made to house three adjacent optical fibers (each 1 mm in diameter) and a single 12 mm diameter, 12 mm focal length plano-convex lens. After fabrication, the design was tested and found to be capable of securing both the fibers and the lens without any permanent adhering of surfaces. The optical housing (15 mm × 25 mm × 22 mm) was precision machined from Delrin® plastic. However, the ball lens (1 mm) were manually glued to the optical fibers (1 mm) using UV curable optical glue. The impact of the manual placement will be discussed later in the paper.

4.4. Information processing

The simplistic nature of the developed L4 response algorithm lends itself to determining the position, velocity and location of a line stimulus within the sensor field of view. It should be emphasized that each sensor cartridge will independently and in parallel using analog processing hardware determine the location of a line stimulus (image edge) within its field of view.

To provide a single signal output from the sensor, the signals from each of the individual photodiodes were combined using the function (L4 output = (left photoreceptor) – (right photoreceptor)). This function was originally proposed by Olson [75], based on the morphological structure of the fly's early vision cells. Olson developed an algorithm that weighted the response from the individual photoreceptors that was then relayed to the L1 and L2 monopolar cells. The difference between the L1 and L2 monopolar cells provided the L4 output. A simple one-dimensional equivalent using three photoreceptors simply takes the difference between the left and the right sensor responses. Figure 4(b) provides the characteristic response for the L4 output for a line stimulus being swept from left to right in front of a one-dimensional sensor as previously described. The center photoreceptor is not used in this specific application but is used in other information processing [76].

Based on the physical structure and dimensions of the sensor, along with the application of basic geometric optical principles, a relationship can be determined between the displacement of a line stimulus within the field of view of the sensor and the corresponding L4 output. Furthermore, if the sensor's field of view is limited between the minimum and maximum L4 responses, a near linear relationship is obtained relating angular stimulus displacement to L4 output [69]. Most importantly, a contrast-invariant response can be

achieved by normalizing the L4 response by the maximum L4 response as the stimulus enters the sensor field of view (FOV). Other contrast-invariant, normalization techniques have been further investigated by Anderson [76]. The circuit producing the L4 response was implemented using standard differential amplifier configuration as shown in figure 4(a) [74].

If an object enters the FOV of the sensor from the right, the initial slope of the signal will be negative. If it enters from the left, the initial slope will be positive (figure 4(b)). By taking the derivative of the signal, it is then possible to determine the direction by which the object entered the field of view. Another possibility is to monitor the L4 (difference) signal and wait for the moment in which the derivative of the signal goes to zero. At this moment, the object has passed through the point where one of the outer photoreceptive elements returns a maximum response. This response provides a definite location of the object in relation to the center of the sensor. By determining the slope of the response as the object passes the point of the maximum response of the initial sensor, it is possible to determine the direction of motion of that object. A negative slope after the initial maximum response point indicates that the object is moving from left to right and a positive slope indicates that the object is moving from right to left.

A simpler solution to the motion problem is within the built-in characteristics of the sensor. The location of an object relative to the center of the sensor is known based upon the peak responses of the left or right sensor elements. By determining which peak has occurred first temporally, it is intuitive that the direction of motion of the object has originated from the direction opposite that of the ball lens sensor that peaks first (due to the image reversal caused by the 12 mm plano-convex lens). For instance, if within a sensor the left ball lens sensor returned a peak response, it would then be known that the object became incident to the FOV of the sensor from the right side. At this point monitoring could continue within the sensor until the right ball lens sensor returned a peak response, confirming the direction of motion of the object.

The determination of velocity of an object is the next logical step in the analysis of the response from the sensor. Since the relationship between the maximum response of the photoreceptors and the angular offset from the center of the lens is known, it is possible to determine when an object has passed one of the maximum response points and when it has passed the second maximum point. Because the radian distance between the two maximum response points is constant and known based on fixed sensor geometry, it is possible to determine the relative speed of the object based upon how much time it takes to pass through each of the maximum response points. Therefore, the velocity of an object passing in front of a sensor can be measured in terms of radians per second. If the range of the object is also known, it would then be possible to determine a linear velocity of the object. If it is possible to determine the location of an object by monitoring the response of the sensor, it then should be possible to determine the range of an object.

Determining the range of an object without prior knowledge of the distance traveled by the object as it passes in front of the sensor is not possible, but if motion were

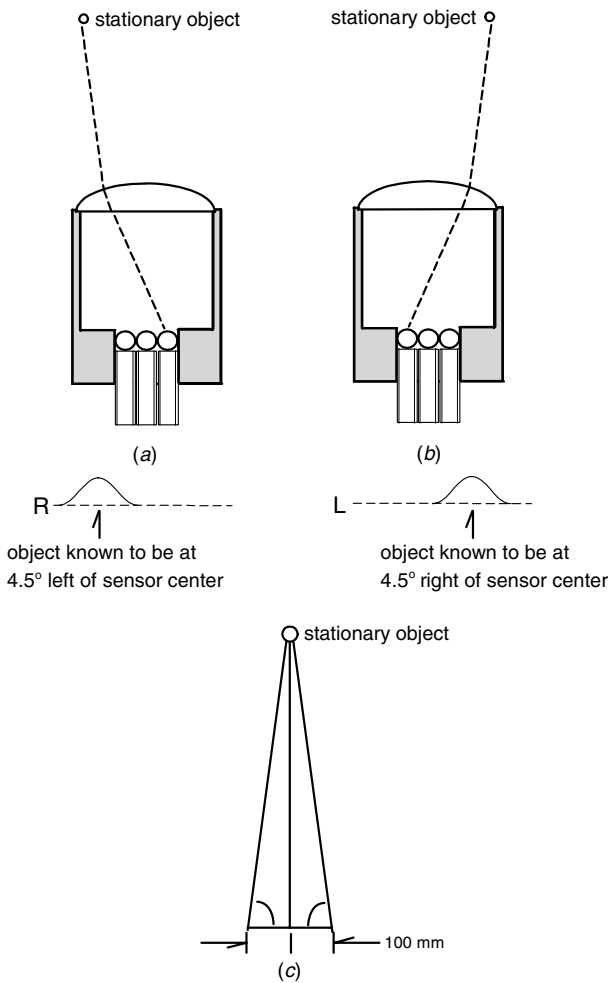


Figure 5. (a) Initial position of the tracked stationary object and the response of the right sensor indicating a position of 4.5° off center to the left of the sensor, (b) final position of the tracked object and the response of the left sensor indicating a position of 4.5° off center to the right of the sensor, and (c) the geometry of the data obtained to determine the range of the object based upon the known angles of incidence and the distance traveled by the sensor platform.

instead initiated by the sensor as it monitored a stationary object, the distance of that object from the sensor can be determined through triangulation. This intentional sensor motion, sometimes called ‘dithering’, is similar to the constant saccadic eye movements of humans and other animals [77]. It is known that the angle an object is offset from the center of the sensor on the left side is approximately 4.5° when the right photoreceptor returns a peak response (figure 5(a)). By moving the platform to the left until the left photoreceptor returns a peak response (figure 5(b)) and precisely measuring the distance the platform traveled, the range of the object can be calculated using simple triangulation. For example, if a line object is detected, a peak response is returned by the right photoreceptor indicating that the object lies at an angle of 4.5° to the left of center. The platform is then moved a distance of 100 mm to the left when the response of the left photoreceptor peaks. It is also known that a peak response from the left

photoreceptor indicates that the object now lies at an angle of 4.5° to the right of the sensor’s center. The data obtained through the motion of the sensor platform can be represented by a triangle (figure 5(c)). Calculating the distance from the plane in which the sensor platform traveled along the object is a matter of applying trigonometric principles. Since the physical architecture of a given sensor is fixed at manufacture, the amount of necessary sensor self-motion to determine the range is determined by the tangent relationship of motion to range. The sensor parameters may be scaled and optimized for a specific application. For this example, the distance of the object from the sensor would be approximately 635 mm for a sensor self-motion of 100 mm. To minimize self-motion, the sensor may take two subsequent position measurements with some known sensor movement between the two readings as opposed to waiting for two peak responses from the sensor.

Aside from sensor movement, this method also implies the requirement for onboard memory as well as the ability to calculate trigonometric functions. Alternatively, two adjacent similarly configured sensors can determine the stimulus range without movement as long as the stimulus is in both sensors’ field of view. This then becomes the familiar triangulation formulation. In this implementation, a memory element is not required; however, the capability to calculate trigonometric functions is still required. This does not preclude the use of an all-analog operational amplifier process; however, the complexity of the processing circuitry will dramatically increase. Depending upon the specific application, a hybrid approach using a combination of analog and digital processing may be used.

5. Testing and results

To test the *Musca domestica* inspired sensor, we designed a battery of experiments and a test platform to perform the tests. The components of this test platform included an oscilloscope for monitoring the signals from the sensor cartridge, a powered breadboard for development of signal conditioning circuitry and a modified X–Y plotter. The modifications to the plotter included the addition of a black shroud to provide a constant background while testing took place. The plotter provides a platform in which movement can be regulated both horizontally and vertically to represent motion as it passes in front of the sensor and distance as it is moved away from the sensor. A line stimulus (wire) was attached to the moveable plotter platform. Since our ultimate goal is a completely passive system, ambient daylight was used as an illumination source. A thorough description of the test configuration is provided by Riley, Harmann and Prabhakara [73, 74, 78].

5.1. Photoreceptor Gaussian profile response

To test the response of a single photodiode configured to mimic the response of the fly’s photoreceptor, the plotter (Houston Instrument Omnigraphic 100 Recorder) was used to slowly (4.33 cm s⁻¹) and constantly move a white strip line stimulus across the sensor’s field of view at a range of 20 cm. A curve

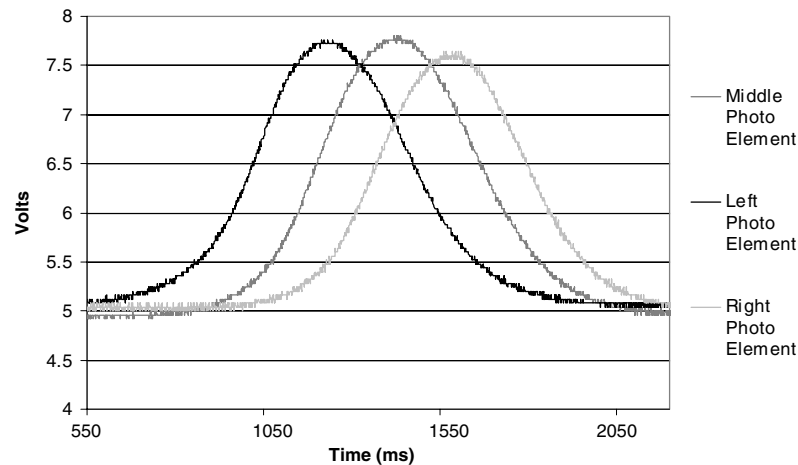


Figure 6. Oscilloscope output for a white object passing through a cartridge sensor field of view at a constant velocity through field of view at 20 cm [85]. The cartridge sensor consists of three bio-inspired photosensors sharing a common main lens.

fitting program (Table Curve 2D version 5.01 [79]) was used to determine the mathematical profile of the test result. The iteratively fit curves were very close to Gaussian curves ($r^2 = 0.994$).

5.2. Overlap of neighboring photo elements

A single sensor consisting of three photosensors sharing a common lens was then tested using the technique described above. Representative results of this test are provided in figure 6. As desired, three nearly identical overlapped Gaussian profiles were obtained. The slight mismatch in Gaussian height was remedied by adjusting the analog gain of the non-inverting amplifier for each photoreceptor to obtain similar profiles. As previously discussed, the amount of overlap required to obtain a vision system with hyperacuity similar to that found in *Musca domestica* was estimated to be between 70% and 80%. The overlap for the tested sensor was measured to be 70%.

5.3. Sensor response to a line stimulus

The sensor's ability to detect small objects was measured by recording a single photo element's response to various sized white line stimuli at different distances from the lens. The first trial tested 25 mm, 14 mm, 7 mm and 1 mm width white strips at a range of 33 cm from the lens (equivalent to 4.33° , 2.43° , 1.2° and 0.174° of arc respectively). The amplifier gain was set to a suitable value and an oscilloscope was used to record the response. The line stimuli were moved across the lens' field of view at a speed of 4.33 cm s^{-1} by the plotter discussed previously. As shown in the test results of figure 7, the sensor was capable of detecting a 1 mm line stimulus at a distance of 33 cm from the lens (0.174° of arc). The next test was performed using the same set of conditions with a fixed 1 mm line stimulus at ranges of 33 cm, 49 cm and 65 cm. The results shown in figure 8 show that at the same gain, the sensor can detect a 1 mm line stimulus at a range of 65 cm (0.088° of arc). Further tests showed that by increasing the

gain of the amplifier, the sensor was capable of detecting the movements of a 1 mm line stimulus at a range of up to 100 cm (0.114° of arc). At the worst case range tested (65 cm), the signal-to-noise ratio (SNR) was approximately 8 dB. As can be seen in figure 8, the resolution of the analog-to-digital converter in the measurement instrument became the limiting case.

5.4. Position determination tests

A line object represented by a white wire was passed in front of the sensor, while the response of the sensor was being monitored by an oscilloscope and two voltmeters. The voltmeters were necessary to monitor the magnitude of the responses and to obtain baseline information on background illumination. The testing was initiated by recording the baseline response of the sensor. The line object was then continuously passed in front of the sensor until a peak response was obtained by the right ball lens sensor. The magnitude of this response was then recorded. The object was then moved a minimal distance and the magnitude of the response was again recorded. This procedure was repeated until the response of the sensor returned to the baseline value. Further investigation had shown that the area between the peak responses was not completely linear as earlier assumed. There are regions of 'roll-off' within the signal due to the Gaussian nature of the photoreceptor responses. Results of a representative test are provided in figure 9. The overall angular error for the data set was 0.036° with a standard deviation of 0.21° . This equates to an average stimulus position error of 0.126 mm with a standard deviation of 0.737 mm at a range of 203 mm.

5.5. Range testing

To test the principles of determining the range of a stationary object, it was necessary to simulate the movement of the sensor platform as to obtain a second view of the object. Given the data from the previous testing, the location of the object is known when the response from either of the photoreceptors

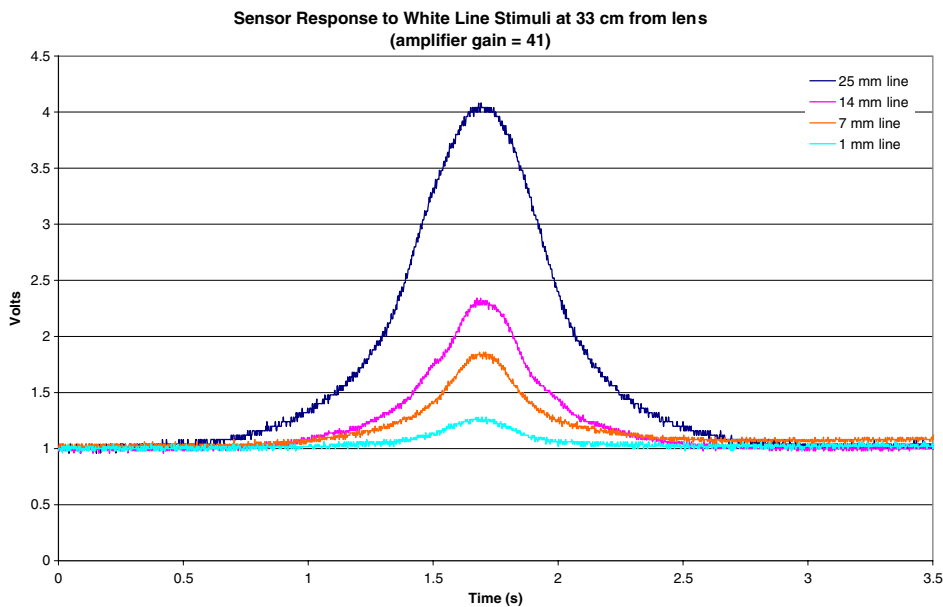


Figure 7. Results for test of a fixed 1 mm line stimulus at various ranges passing through a cartridge sensor field of view at a constant velocity [85]. The cartridge sensor consists of three bio-inspired photosensors sharing a common main lens.

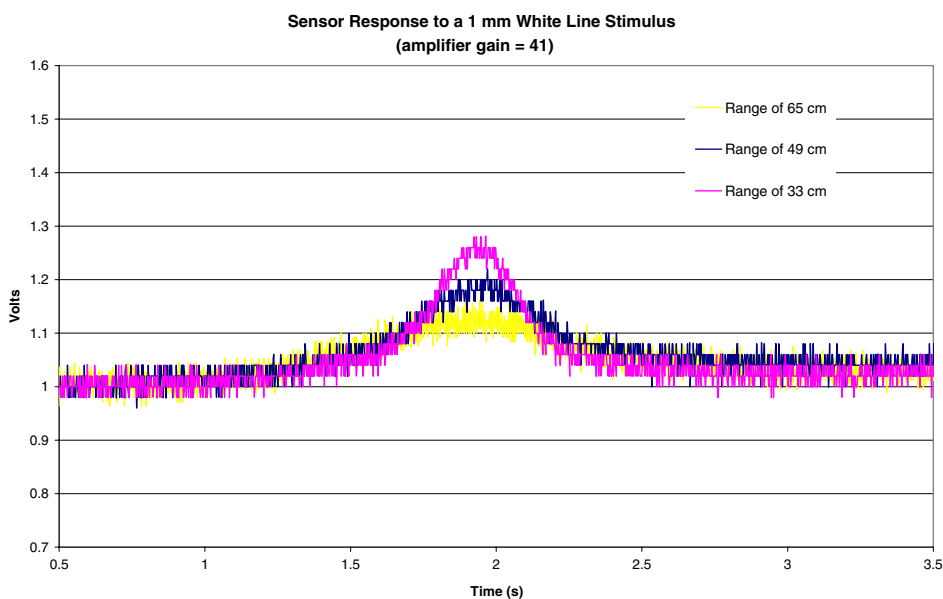


Figure 8. Results for test of a fixed 1 mm line stimulus at various ranges at various ranges passing through a cartridge sensor field of view at a constant velocity [85]. The cartridge sensor consists of three bio-inspired photosensors sharing a common main lens. The resolution of the analog-to-digital converter in the measurement instrument became the limiting case.

peaks. By measuring the distance traveled by the sensor, it is then possible to determine the range of the object by applying trigonometric calculations as described previously. Since only relative motion is important, and the sensor was in a fixed test setup, we chose to simulate the movement of the sensor by moving the object instead. The distance traveled by the object between the peak responses of the photoreceptors was used to indicate the distance traveled by the sensor as if it was mounted on a stationary object. To calculate the perceived

range of the object, simple geometry was employed. Since the object was moved instead of the sensor for purposes of this test, calculations were based upon the movement of the object in reference to the sensor and the distance of the sensor from the object was calculated. The distance calculated would be from the object to the focal point of the sensor. The angles used to calculate the range would be those determined by the object location tests. Since these angles varied slightly between the left and right ball lens measurements and average of the values

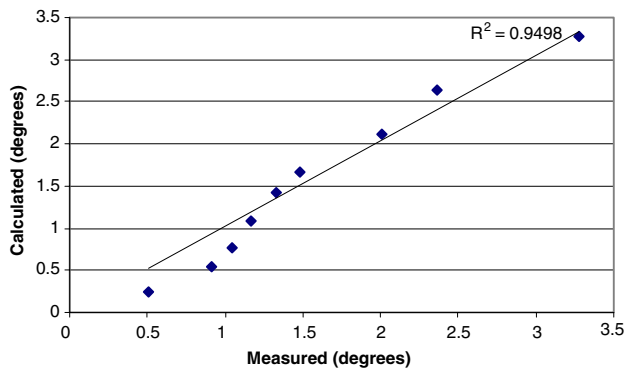


Figure 9. Calculated versus measured angular offsets of a 1 mm line stimulus at a range of 203 mm localized using a bio-inspired cartridge sensor. The cartridge sensor consists of three bio-inspired photosensors sharing a common main lens.

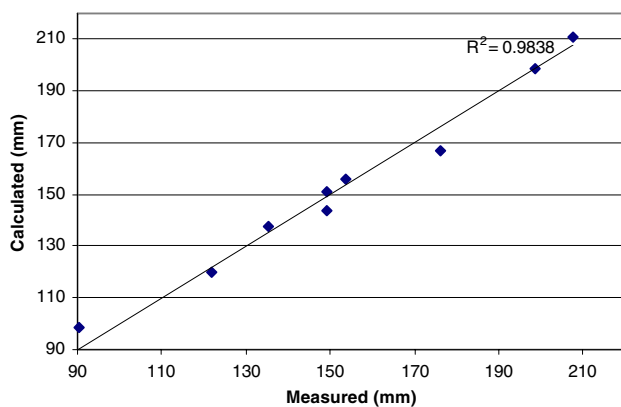


Figure 10. Average of the calculated range values from the right and left ball lens sensors of a cartridge sensor as compared to the measured values of the actual range.

were used to calculate the sensor range. Results are provided in figure 10. The overall range error for the data set was 5.5 mm with a standard deviation of 3.63 mm.

It must be emphasized that even in contrast-varying situations, the shape of the sensor response will remain constant. That is, the location of the peak responses within the signal will always occur in the same location. This allows for the simple tracking of peak values from the left-most and right-most photoreceptors in the sensor to obtain the range. These principles can be applied to an array of sensors to determine the range of a moving object and stationary platform. In an array of sensors, the physical distance between sensor elements is a known factor. Location information is available as the object passes by each sensor in the array. Therefore, if two separate sensors in the array capture location information concerning the object, it is then possible to apply the same procedures outlined above to calculate the range of the moving object from the stationary array.

5.6. Follow-on testing

Additional testing and modeling of the described sensor has been accomplished under a variety of stimulus widths, contrast

and lighting conditions, and also in a noisy environment. These results are reported elsewhere [76, 78, 80]. Anderson’s work will be covered in detail in a subsequent article for this journal.

6. Discussion

There are a number of sources of error for a sensor configuration of this type. Each will be discussed in turn.

- (i) We have assumed a linear response for the difference term for the right photoreceptor response and the left photoreceptor response. The difference between two Gaussian-shaped profiles are actually quasi-linear when examined between the peak values. The variation from the linear response is more pronounced at the peak of the difference waveform. The impact of the quasi-linear response may be minimized by insuring enough overlap between the Gaussian profiles.
- (ii) For the individual photoreceptors, a 1 mm ball lens was manually affixed to a 1 mm optical fiber using UV curable glue. Any misalignment between the ball and the fiber will result in an induced error in determining the stimulus position and range.
- (iii) We have positioned the focal point of the main lens at the focal point of the center ball lens. We have assumed that the image is in focus at the focal point of the lens. The thin lens equation indicates that this assumption is valid when the object is at a distance from the lens far greater than the focal point of the lens [81]. Sensitivity analysis of this consideration indicates that for ranges less than 100 mm for the tested configuration, significant errors will result. This causes short-range limitations.
- (iv) At long ranges, the limiting factor is the ability to distinguish the stimulus from its background. This is a combined effect of the stimulus and background contrast as well as the resolution of the analog-to-digital converter employed in the measurement. Prabhakara and Anderson have studied the contrast effects in detail [76, 78, 80].

Even with all of these error sources taken into account, we were able to localize a 1 mm line stimulus at a range of 203 mm with an overall angular error for the data set of 0.036° with a standard deviation of 0.21° . This equates to an average stimulus position error of 0.126 mm with a standard deviation of 0.737 mm at a range of 203 mm. We were also able to determine the range of the stimulus with an overall range error for the data set of 5.5 mm with a standard deviation of 3.63 mm. Furthermore, all error sources are well understood and may be characterized and compensated for in a specific application.

7. Summary and conclusions

A sensor has been developed, inspired by the early processes of the fly’s vision system. It is important to emphasize some of the key attributes of this sensor.

Basic feature detector. The sensor is able to detect and localize a line stimulus in two-dimensional space. We are already

extending this work to the recognition and localization of other image tokens such as edges and spots.

Parallel. Each sensor cartridge is self-contained, although it has the capability to share information with its nearest neighbors. This allows development of an array of such sensors, all operating in parallel.

Continuous, analog operation. The sensor provides continuous output. Information may be tapped off from individual photoreceptors or the various operational amplifier outputs. As previously mentioned, all-analog processing or hybrid analog/digital processing should be carefully considered for the application at hand.

Passive. The system is entirely passive in operation. That is, it emits no source of radiant energy. This can be an extremely important attribute, particularly in sensitive applications.

Contrast invariant. Due to the normalization of sensor output characteristics, the sensor provides identical outputs under varying contrast conditions between the stimulus and the background with a very wide range. Recently, Prabhakara *et al* characterized the sensor under widely varying contrast environments. It was demonstrated that the sensor continues to operate even when a black line stimulus is swept across a black background [78, 80]. Anderson has also studied alternative methods of contrast variation [76].

Simple response. The sensor is quite simple in design using standard optical and operational amplifier components.

Scalable. The sensor geometry is scalable. It can be employed at the VLSI level as well as in large-scale sensors. A second VLSI scale prototype consisting of seven cartridges and seven photoreceptors is currently under development [9, 82].

Sensor overlap. Due to the overlapping Gaussian field of views (FOVs) within the sensor, an object is never 'lost between pixels' once it enters the field of view. Furthermore, an array of such sensors would all have overlapping FOVs such that an object would not be 'lost' across the entire face of the array.

2D sensor. The lessons learned with the one-dimensional sensor may be extended to a 2D and even a 3D sensor much like the vision system of the fly. We have extensively modeled an array of 10 000 interacting 2D sensors. There is much information to be exploited here. We have already demonstrated the capability to generate flow field data using temporal information. This allows for higher level image processing procedures such as segmentation and tracking. We are also working to integrate the sensor technology with existing and new object recognition algorithms [76, 83].

Fabrication. The sensors used in this study were 'handmade'. The fabrication of a prototype 2D sensor would be significantly challenging if we continued the use of a ball lens and fiber to obtain the overlapping Gaussian profile. We are currently fabricating a sensor prototype consisting of seven ommatidia with seven photoreceptors, each using standard off-the-shelf photodiodes. The photodiodes were specifically chosen to provide overlapping Gaussian profiles (OPTTEK 906). Use of this photodiode will replace the need for optical fibers for larger

scale sensors. Furthermore, recent work by Lee and Jeong have demonstrated the feasibility of using machine processing to fabricate ommatidia in an omnidirectional arrangement along a hemispherical polymer dome such that they provide a wide field of view similar to that of a natural compound eye [56, 84].

The sensor technology described in this paper would find wide application in a variety of medical, commercial, industrial and defense applications. For example, the military has identified a need for better robotic vision to be incorporated into unmanned vehicles, unmanned aerial vehicles or guided weapons such as missiles. The sensor design approach we have described shows promise for these applications due to its potential for complete analog processing, passive operation and the capability to be scaled to integrated circuit size applications. The sensor would also be a potential candidate for high speed inspection as found in production industry or detecting inconsistencies in overhead power lines or track inconsistencies in commercial rail line applications. We envision this new sensor as a supplement to more traditional imaging sensors for most applications, and not as a replacement. Just as *Musca domestica* has both two compound eyes and a very simple camera eye, many computer and robot vision tasks can benefit from both types of sensors.

Acknowledgments

This research was sponsored in part by National Institute of Health (NIH) Center of Biomedical Research Excellence (COBRE) Grants. Specifically, this publication was made possible by grant numbers P20 RR015553, RR15640 and P20 RR15640 from the National Center for Research Resources (NCR), a component of the National Institutes of Health (NIH). Its contents are solely the responsibility of the authors and do not necessarily represent the official views of NCR or NIH. An early version of this paper was presented at the Smart Sensor Technology and Measurement Systems Conference, Smart Structures and Materials Symposium, SPIE—The International Society for Optical Engineering, March 2005, San Diego, CA [85]. The authors would also like to thank Dr Michael Wilcox, Department of Biology, United States Air Force Academy, Colorado for his continued technical expertise and advice. The authors would also like to thank John A (Tony) Nevshemal, former director, University of Wyoming Research Products Center; Brian D Owens, Intellectual Property Analyst; and Davona Douglas, JD for their assistance in establishing patent protection procedures for this concept and related products.

References

- [1] Liu P and Thompson D 2001 *IEEE 1394: Changing the Way We Do Multimedia Communications* IEEE Computer Society, 2 May 2001, <http://computer.org/multimedia/articles/firewire.htm>, 2 May 2001
- [2] Mazokhin-Porshnyakov G A 1969 Structure of faceted eyes and visual centers *Insect Vision* (New York: Plenum) pp 1–26

- [3] Hardie R C, Franceschini N, Ribi W and Kirschfeld K 1981 Distribution and properties of sex-specific photoreceptors in the fly *Musca domestica* *J. Comp. Physiol.* **145** 139–52
- [4] Braitenberg V and Debbage P 1974 A regular network of reciprocal synapses in the visual system of the fly *Musca domestica* *J. Comput. Physiol.* **90** 25–31
- [5] Braitenberg V 1967 Patterns and projection in the visual system of the fly: I. Retina-lamina projections *Exp. Brain Res.* **3** 271–98
- [6] Snyder A W, Bossomaier T R J and Hughes A 1986 Optical image quality and the cone mosaic *Science* **231** 499–501
- [7] Tomberlin E 2004 *Musca domestica*'s large monopolar cell responses to visual stimuli *Thesis* The University of Wyoming
- [8] Juusola M and French A S 1997 Visual acuity for moving objects in first- and second-order neurons of the fly compound eye *J. Neurophysiol.* **77** 1487–95
- [9] Wilcox M and Thelen D 1999 A retina with parallel input and pulsed output, extracting high-resolution information *IEEE Trans. Neural Netw.* **10** 574–83
- [10] Coombe P E, Srinivasan M V and Guy R G 1989 Are the large monopolar cells of the insect lamina the optomotor pathway? *J. Comput. Phys. A* **166** 23–35
- [11] Douglass J K and Strausfeld N J 2001 Pathways in dipteran insects for early visual motion processing *Motion—Computational, Neural, and Ecological Constraints* ed J M Zanker and J Zeil (Berlin: Springer) pp 67–81
- [12] Strausfeld N J and Campos-Ortega J A 1977 Vision in insects: pathways possibly underlying neural adaptation and lateral inhibition *Science* **195** 894–7
- [13] Strausfeld N J and Campos-Ortega J A 1973 The L4 monopolar neurone: a substrate for lateral interaction in the visual system of the fly *Musca domestica* (L.) *Brain Res.* **59** 97–117
- [14] van Hateran J H 1986 Electrical coupling of neuron-ommatidial photoreceptor eyes *J. Comput. Physiol. A* **158** 795–811
- [15] van Hateran J H 1989 Photoreceptor optics theory and practice *Facets of Vision* (Berlin: Springer)
- [16] van Hateran J H 1987 Neural superposition and oscillations in the eye of the blowfly *J. Comput. Physiol. A* **161** 849–55
- [17] van Hateran J H 1984 Waveguide theory applied to optically measured angular sensitivities of fly photoreceptors *J. Comput. Physiol. A* **154** 761–71
- [18] van Hateran J H 1992 Theoretical predictions of spatiotemporal receptive fields of fly LMCs, and experimental validation *J. Comput. Physiol. A* **171** 157–170
- [19] Stavenga D G 2003 Angular and spectral sensitivity of fly photoreceptors. I Integrated facet lens and rhabdomere optics *J. Comput. Physiol. A* **189** 1–17
- [20] Stavenga D G, Franceschini N and Kirschfeld K 1984 Fluorescence of housefly visual pigment *Photochem. Photobiol.* **40** 653–9
- [21] Stavenga D G, Kinoshita M and Yang E C 2001 Retinal regionalization and heterogeneity of butterfly eyes *Naturwissenschaften* **88** 477–81
- [22] Nakayama K 1985 Biological image motion processing: a review *Vis. Res.* **25** 625–60
- [23] Arnett D W 1972 Spatial and temporal integration properties of units in first optic ganglion of dipterans *J. Neurophysiol.* **35** 429–44
- [24] Pick B 1977 Specific misalignments of rhabdomere visual axes in the neural superposition eye of dipteran flies *Biol. Cybern.* **26** 215–24
- [25] Wilcox M 1994 Structure and function of gap junctions in the photoreceptor axon terminals of the fly *Biomembrane Electrochemistry* (Washington, DC: American Chemical Society)
- [26] Bucklew J A and Saleh B E A 1985 Theorem for high-resolution high-contrast image synthesis *J. Opt. Soc. Am. A* **2** 1233–6
- [27] Bruce V and Green P 1985 *Visual Perception—Physiology, Psychology, and Ecology* (Hillsdale: Laurence Erlbaum Associates)
- [28] Reichardt W 1969 Movement perception in insects *Proc. Int. School of Physics, Enrico Fermi, Processing of Optical Data by Organisms and Other Machines* (London: Academic) pp 465–93
- [29] Harrison R R and Koch C 2000 Silicon implementation of the fly's optomotor control system *Neural Comput.* **12** 2291–304
- [30] Higgins C M and Shams S A 2002 A biologically inspired modular VLSI system for visual measurement of self motion *IEEE Sensors J.* **2** 508–28
- [31] Horridge G A 1990 A template theory to relate visual processing to digital circuitry *Proc. R. Soc.* **239** 17–33
- [32] Liu S 2000 A neuromorphic a VLSI model of global motion processing in the fly *IEEE Trans. Circuits Syst. II* **47** 1458–67
- [33] Moini A, Bouzerdoum A, Eshraghian K, Yakovlev A, Nguyen X T, Blansky A, Beare R, Abbott D and Bogner R E 1997 An insect vision-based motion detection chip *IEEE J. Solid-State Circuits* **32** 254–79
- [34] Netter T and Franceschini N 2002 A robotic aircraft that follows terrain using a neuromorphic eye *Proc. IEEE/RSJ* 129–34
- [35] Omgen H and Gagne S 1990 Neural network architectures for motion perception and elementary motion detection in the fly visual system *Neural Netw.* **3** 487–505
- [36] Anonymous 2008 Max Planck Institute for Biological Cybernetics. Max Planck Society <http://www.kyb.tuebingen.mpg.de/>
- [37] Abbott D 2008 *Adelaide Insect Vision Group* University of Adelaide, <http://www.eleceng.adelaide.edu.au/Groups/Bugeye>
- [38] Strausfeld N 2008 *The Strausfeld Laboratory* University of Arizona, <http://web.neurobio.arizona.edu/Lab/>
- [39] O'Carroll D 2008 *Insect Vision Research* University of Adelaide, <http://www.eleceng.adelaide.edu.au/personal/davidoc/projects.html>
- [40] Barlow H B 1953 Summation and inhibition in the frog's retina *J. Physiol.* **199** 69–88
- [41] Lettvin J Y, Maturana R R, McCulloch W S and Pitts W H 1959 What the frog's eye tells the frog's brain *Proc. Inst. Radiat. Eng.* **47** 1940–51
- [42] Hubel D H and Weisel T N 1979 Brain mechanisms of vision *Sci. Am.* **241** 150–62
- [43] Marr D 1982 *Vision: A Computational Investigation into the Human Representation and Processing of Visual Information* (New York: Freeman)
- [44] Nakayama K and Loomis J M 1974 Optical velocity patterns velocity sensitive neurons, and space perception: a hypothesis *Perception* **3** 63–80
- [45] O'Carroll D C 1993 Feature detecting neurons in Dragonflies *Nature* **362** 541–3
- [46] Laughlin D C 1997 Spatio-temporal properties of motion detectors matched to low image velocities in hovering insects *Vis. Res.* **37** 3427–39
- [47] Zheng L, de Polavieja G G, Wolfram V, Asyali M H, Hardie R C and Juusola M 2006 Feedback network controls photoreceptor output at the layer of first visual synapses in *Drosophila* *J. Gen. Physiol.* **127** 495–510
- [48] Reichardt W 1961 *Autocorrelation, A Principle for the Evaluation of Sensory Information by the Central Nervous System Sensory Communication* ed W A Rosenblith (New York: Wiley)

- [49] Srinivasan M and Dvorak D 1980 Spatial processing of visual information in the movement-detecting pathway of the eye *J. Comput. Physiol. A* **140** 1–23
- [50] Bishop L G, Keehn D G and McCann G D 1968 Studies on motion detection by interneurons of the optic lobes and brains of the flies *Calliphora Phaenicia* and *Musca domestica* *J. Neurophysiol.* **31** 509–25
- [51] Land M F 1997 Visual acuity in insects *Ann. Rev. Entomol.* **42** 147–77
- [52] Moses K 2006 Fly eyes get the whole picture *Nature* **442** 638–9
- [53] Bruckner A, Duparre J and Brauer A 2007 Position detection with hyperacuity using artificial compound eyes *Proc. SPIE—Sensors, Cameras, and Systems for Scientific/Industrial Applications VIII* vol 6501 65010D
- [54] Sanders J S and Halford C E 1995 Design and analysis of apposition compound eye optical sensors *Opt. Eng.* **34** 222–35
- [55] Rosen J and Abbokasis D 2003 Seeing through biological tissues using the fly eye principle *Opt. Express* **11** 3605–11
- [56] Jeong K, Kim J and Lee L P 2006 Biologically inspired artificial compound eyes *Science* **312** 557–61
- [57] Currin M S 1994 Design aspects of multi-apertures vision system point trackers that use apposition eyelets *Thesis* The University of Memphis
- [58] Tanida J, Kumagai T, Yamada K, Miyatake S, Ishida K, Morimoto T, Kondou N, Miyazaki D and Ichioka Y 2001 Thin observation module by bound optics (TOMBO): concept and experimental verification *Appl. Opt.* **40** 1806–13
- [59] Tunida J 2003 Color imaging with an integrated compound imaging system *Opt. Express* **11** 2109–17
- [60] Horisaki R, Irie S, Ogura Y and Tanida J 2007 Three-dimensional information acquisition using a compound imaging system *Opt. Rev.* **14** 347–50
- [61] Hoshino K, Mura F and Shimoyama I 2001 A one-chip scanning retina with an integrated micro-mechanical scanning actuator *J. Micromech. Syst.* **10** 492–7
- [62] Harrison R R and Koch C 2000 A robust analog VLSI Reichardt motion sensor *Analog Integr. Circuits Signal Process.* **24** 213–29
- [63] Harrison R R and Koch C 1998 An analog VLSI model of the fly elementary motion detector *Advances in Neural Information Processing Systems* vol 10 ed M I Jordan, M J Kearns and S A Solla (Boston: MIT Press)
- [64] Harrison R R 2005 A biologically inspired analog IC for visual collision detection *IEEE Trans. Circuits and Syst. I* **52** 2308–18
- [65] Harrison R R and Koch C 2000 A silicon implementation of the fly's optomotor control system *Neural Comput.* **12** 2291–304
- [66] Pudas M, Viollet S, Ruffier F, Krusing A, Amic S, Leppavuori S and Franceschini N 2007 A miniature bio-inspired optic flow sensor based on low temperature co-fired ceramics (LTCC) technology *Sensors Actuators* **133** 88–95
- [67] Anonymous 2008 Plastic fiber optic IRLEDS-IFE91A. Industrial Fiber Optics Inc. <http://www.i-fiberoptics.com/>
- [68] Clark T and Wanser K 2008 *Choosing Ball or GRIN Lenses* (Deposition Sciences Inc.) <http://www.depsci.com>
- [69] Kennedy T P 2008 *Understanding Ball Lenses* Edmund Industrial Optics <http://www.edmundoptics.com>
- [70] Garcia K J 2000 Calculating component coupling coefficients *WDM Solutions, Supplement of Laser Focus World* (Chatsworth, CA: Pen Well Corporation)
- [71] Upton R S and Koshel R J 2000 Modeling coherent propagation aids accurate coupling *WDM Solutions, Supplement of Laser Focus World* (Chatsworth, CA: Pen Well Corporation)
- [72] Anonymous 2008 TSL250R, TSL251R, and TSL252R light-to-voltage optical sensors Texas Advanced Optoelectronic Solutions, <http://www.taosinc.com/>
- [73] Harman W M 2005 Biomimetic analog machine vision system characterization and application *Thesis* College of Engineering, University of Wyoming
- [74] Riley D 2004 *Musca domestica's* inspired machine vision *Thesis* College of Engineering, University of Wyoming
- [75] Olson T E 2001 Biologically based machine vision: modeling the L1, L2, L4 neurons of the housefly (*Musca domestica*) vision system *Thesis* College of Engineering, University of Wyoming
- [76] Anderson T M 2007 Motion detection algorithm based on the common housefly eye *Thesis* College of Engineering, University of Wyoming
- [77] Barlow H B and Mollon J D 1984 *The Senses* (London: Cambridge University Press)
- [78] Prabhakara R S, Wright C H G, Barrett S F and Harman W M 2006 Quantitative and qualitative performance comparison of a biomimetic vision sensor with commercial CCD camera sensors *Proc. SPIE 18th Int. Symp. on Electronic Imaging (SPIE 6068-16)* (January 2006)
- [79] Anonymous 2008 Table curve 2D version 5.01 Systat Software, Inc. www.systat.com/products/tablecurve2d/
- [80] Prabhakara R S 2006 Quantitative and qualitative performance comparison of a biomimetic vision sensor with commercial CCD camera sensors *Thesis* College of Engineering, University of Wyoming
- [81] Miller F 1977 *College Physics* 4th edn (New York: Harcourt Brace)
- [82] Cox D 2003 Fly eye program *Cadel Microelectronics*
- [83] Madsen R N 2005 Software model of a machine vision system inspired by the common housefly *Thesis* College of Engineering, University of Wyoming
- [84] Lee L P and Szema R 2005 Inspirations from biological optics for advanced photonic systems *Science* **310** 1148–50
- [85] Riley D T, Harman W H, Tomberlin E, Barrett S F, Wilcox M and Wright C H G 2005 *Musca domestica* inspired machine vision system with hyperacuity *Proc. SPIE Smart Sensor Technology and Measurement Systems Conf., Smart Structures and Materials Symposium (San Diego, CA, March 2005)* vol 5758, pp 304–20